Reports

Kinetics of the Fe^{2+}-Mg, Order-Disorder Reaction in Anthophyllites: Quantitative Cooling Rates

Abstract. *The kinetics of the* Fe^{2+}*-Mg, order-disorder phenomenon in a highly ordered natural anthophyllite have been determined over the temperature range from 400° to 720°C at a pressure of 2 kilobars. At temperatures of 600°C and above, equilibrium is attained by disordering as well as ordering reactions. The intracrystalline exchange is defined by a standard Gibbs free energy of 4247 ± 54 calories per formula unit. Rate studies at 550° and 500°C show that equilibrium is attained by ordering but not by disordering within the same time scale and that the exchange reaction is characterized by an activation energy of ~55 kilocalories per formula unit. An equilibration temperature for the natural anthophyllite of 270°C is determined from the termination of the ordering process owing to excessively slow reaction kinetics after* $\sim 10^7$ *years. From the rate constants of the exchange process, for different crystallization temperatures, the apparent equilibration temperature of 270°C defines a maximum linear cooling rate for the rock of* 1×10^{-4} *°C per year.*

The kinetics of the order-disorder phenomenon in silicates potentially offers a unique tool for the quantitative determination of the equilibrium cooling history of natural crystals. It is well known from site population measurements by means of x-ray structure refinements and ^{57}Fe Mössbauer studies that the intracrystalline equilibria in natural chain silicates often correspond to temperatures at which the ordering of cations between crystallographically distinct sites is terminated during cooling of the rock system. It is inferred, however, that the temperature below which further ordering does not occur (the cutoff temperature), even on a geological time scale, is the rather high value of approximately 480°C (*1–3*). To explain these results, Mueller (*4*) postulated a mechanism consisting of two consecutive steps involving a high-temperature process with an activation energy of ~20 kcal/mole and a low-temperature process, below the cutoff temperature, characterized by a significantly higher activation energy. In these terms, the cutoff temperature or thermal barrier is explained in terms of a drastic reduction of the rate constants at temperatures below ~480°C. Furthermore, values for the rate constant at temperatures slightly above the thermal barrier appear to be close to zero, at least within the experimental errors (*5*), and this situation precludes calculation of the cooling history of natural crystals. We report here new insight into the nature of this low-temperature thermal barrier which has been obtained from studies of the kinetics of the order-disorder reaction in an orthorhombic amphibole, anthophyllite [Rabbitt sample 30 (*6*)].

Topologically, the amphibole crystal structure consists of octahedral MO_6 strips sandwiched between double chains of silica tetrahedra parallel to the crystallographic *c* direction. There are four nonequivalent octahedral sites, designated $M1^8$, $M2^8$, $M3^4$, and $M4^8$ (the superscripts refer to the site multiplicity per unit cell). The average electron microprobe analysis of Rabbitt sample 30 gave the structural formula $Na_{0.05}Ca_{0.09}Mg_{5.79}Fe^{2+}{}_{1.17}Si_{7.87}Al_{0.18}O_{22}(OH)_2$, suggesting an edenite-like substitution, with Na substituting in the normally vacant A sites and Al^{3+} replacing Si in the tetrahedrally coordinated sites (*7*). Trivalent iron was not detected in the natural sample by the Mössbauer technique, and the inferred charge imbalance may reflect loss of Na during the electron microprobe analysis. This sample was chosen because the three-dimensional x-ray structure refinement (*8*) showed that it has no exsolution features and also that it is highly ordered, the atomic fraction X^{Fe} [equal to $Fe^{2+}/(Fe^{2+} + Mg)$] being high in the M4 positions ($X^{Fe}{}_{M4} = 0.651$); low in the M1, M2, and M3 sites (weighted average in the five positions, $X^{Fe}{}_{M1,M2,M3} = 0.034$); and not substantially partitioned between the latter five positions. The sample is from within an ultramafic body in Montana and occurs together with actinolite, serpentine, enstatite, clinohumite, spinel, annabergite, and magnetite (*6*).

The kinetic experiments were carried out in the temperature range from 400° to 720°C and a pressure of 2 kbar in standard cold-seal pressure vessels and at oxygen fugacities defined by the fayalite-magnetite-quartz buffer. The equilibrium data were independent of the presence or absence of a hydrous vapor phase during the heating process. The upper temperature of the experiments is of course limited because anthophyllite is unstable above ~750°C and 2 kbar, decomposing to orthopyroxene plus quartz (*9*).

We used the ^{57}Fe Mössbauer technique to monitor the Fe^{2+}-Mg exchange between sites because of the rapidity of the technique and because the precision of the Fe^{2+} site occupancies is of the order of ±0.005. Experimental details are similar to those of Hafner and Ghose (*10*). It should be noted, however, that the ^{57}Fe absorption spectrum at 77°K consists of two well-resolved quadrupole split doublets, an inner doublet corresponding to Fe^{2+} in the M4 position and an unresolved outer doublet due to Fe^{2+} in the M1, M2, and M3 sites. The ratios of the areas of the respective absorption doublets are taken as proportional to the ratio of Fe^{2+} between the two M4 sites and the total of five M1 + M2 + M3 sites per unit cell, and these ratios are converted to Fe^{2+} site occupancy numbers (Table 1) (*3*). The Mg occupancy numbers are determined by difference, on the assumption that the M sites are fully occupied by Fe^{2+} and Mg (*11*).

The order-disorder relationship studied is the Fe^{2+}-Mg exchange between M4 and the other M sites, represented by the equilibrium

$$\mathrm{Mg_{M1,M2,M3}} + \mathrm{Fe^{2+}{}_{M4}} \rightleftarrows \mathrm{Fe^{2+}{}_{M1,M2,M3}} + \mathrm{Mg_{M4}} \qquad (1)$$

The results presented in this report can be fitted by the rate equation for a second-order competing rate process (*12*), assuming a Fe^{2+}-Mg binary solid solution (*11*),

$$-\frac{dX_4}{dt} = C_0 \frac{5}{7} \phi_{4\text{-}123} k_{4\text{-}123} X_4 (1 - X_{123}) - C_0 \frac{5}{7} \phi_{123\text{-}4} k_{123\text{-}4} (X_{123}) (1 - X_4) \qquad (2)$$

where X_4 and X_{123} are the Fe^{2+} site occupancy values; k_{4-123} and k_{123-4} are the respective rate constants for disordering and ordering, ϕ_{4-123} and ϕ_{123-4} are the activity coefficients and relate to the ideality of mixing on the respective sites, and C_0 is the total concentration of all sites per unit volume of the crystal. Equation 2 can be reduced to a logarithmic decay for one-site occupancy with time (*13*) by substitution of the equilibrium constant, $K^{\circ}_{123\text{-}4}$, and the bulk X^{Fe} value, namely,

$$K^{\circ}_{123\text{-}4} = \frac{X_4(1 - X_{123})}{X_{123}(1 - X_4)} = \frac{k_{123\text{-}4}}{k_{4\text{-}123}} = \frac{1}{p} \qquad (3a)$$

where p is the ordering parameter, and

$$X_{123} = \frac{7}{5} X^{\mathrm{Fe}} - \frac{2}{5} X_4 \qquad (3b)$$

and assuming ideal mixing on the sites, namely, $\phi_{123\text{-}4} = \phi_{4\text{-}123} = 1$. The resultant equation takes the form:

$$-\frac{dX_4}{dt} = k_{4\text{-}123}(cX_4^2 + bX_4 + a) \qquad (4)$$

where

$$a = -K^{\circ}_{123\text{-}4} X^{\mathrm{Fe}}$$

$$b = K^{\circ}_{123\text{-}4} X^{\mathrm{Fe}} - X^{\mathrm{Fe}} + \frac{2}{7} K^{\circ}_{123\text{-}4} + \frac{5}{7}$$

and

$$c = \frac{2}{7}(1 - K^{\circ}_{123\text{-}4})$$

From Eq. 4 and using isothermal values of X_4 at known times, one can determine the isothermal rate constants.

At temperatures of 600°C and above, an equilibrium distribution (*14*) is attained within a few days in both wet and dry runs as demonstrated by the disordering rate studies and a reversal experiment at 600°C in which the starting material for the ordering experiment was initially disordered at 720°C for 1 day. The equilibrium constants found at 600°, 670°, and 720°C (Table 1) define a constant value of the standard Gibbs free energy, $\Delta G^{\circ}_{\mathrm{ex}}$, of 4247 ± 54 cal/formula unit. One can conclude from these results that an ideal exchange between the sites was attained. On the assumption that this relationship holds at lower temperatures, the Fe^{2+}-Mg distribution in the natural anthophyllite ($X^{\mathrm{Fe}}{}_{\mathrm{M4}} = 0.533$) corresponds to a temperature of ~270°C. This temperature is substantially lower than the cutoff temperature (~480°C) inferred for natural orthopyroxenes (*1*) and cummingtonite-grunerite solid solutions (*2, 3, 10*). A quantitative interpretation of this low temperature of equilibrium for the natural sample can be deduced from detailed rate studies at 550° and 500°C, starting from natural and previously disordered crystals (720°C for 1 day).

Table 1. Equilibrium values of the ordering parameter, p, and the standard Gibbs free energy exchange, $\Delta G^{\circ}_{\mathrm{ex}}$.

Sample (°C kbar^{-1} day^{-1})	p*	$\Delta G^{\circ}_{\mathrm{ex}}$† (cal/mole)
720/2/4	0.1205 (5)	4175
670/2/9	0.1050 (1)	4223
600/2/15	0.0855 (2)	4266
720/2/1 + 550/2/24‡	0.0721 (3)	4300

*Values of p are calculated from Eq. 3a. The site occupancy values are calculated from $X^{\mathrm{Fe}}{}_{\mathrm{M}_4} = 7/2\, X^{\mathrm{Fe}}[1 = (A_1 + A_2)/(A_1 + A_2 + B_1 + B_2)]$ and $X^{\mathrm{Fe}}{}_{\mathrm{M}_1,\mathrm{M}_2,\mathrm{M}_3} = 7/5\, X^{\mathrm{Fe}}[(A_1 + A_2)/(A_1 + A_2 + B_1 + B_2)]$, where X^{Fe} is the atomic fraction $\mathrm{Fe}^{2+}/(\mathrm{Fe}^{2+} + \mathrm{Mg})$ in anthophyllite and $(A_1 + A_2)$ and $(B_1 + B_2)$ are, respectively, the sum of the areas of the outer absorption doublet due to the average Fe^{2+} in sites M1, M2, and M3 and the inner absorption doublet due to Fe^{2+} in site M4 (*2, 3, 10, 14*). Numbers in parentheses refer to the number of replicate absorption determinations. †Calculated from the relationship $\Delta G^{\circ}_{\mathrm{ex}} = -RT \ln p$, where R is the gas constant and T is the absolute temperature. ‡The intrinsic equilibrium state for the disordering experiment 550/2/26 is characterized by $p = 0.0553$.

For example, the rate studies at 550°C confirm the second-order rate equation (*14*), and the equilibrium Fe^{2+}-Mg distribution obtained after ordering for 24 days ($p = 0.072$, Table 1) gives a $\Delta G^{\circ}_{\mathrm{ex}}$ value in close agreement with the values obtained at higher temperatures (Table 1). Significantly, however, equilibrium is not reached by disordering the natural material at 550°C for 26 days (Table 1). The rate constants, $k_{4\text{-}123}$, determined at 550° and 500°C are given in Table 2. The disordering rate constants calculated from the ordering experiments are larger than those calculated from the disordering experiments. This difference might be explained as resulting from some degree of nonideal mixing in the cation sites, namely, $\phi_{ij} \neq \phi_{ji} \neq 1$ in Eq. 2. Nevertheless, the activation energies for the rate process calculated from the disordering and ordering data, 55 and 62 kcal/mole, respectively, are not significantly different.

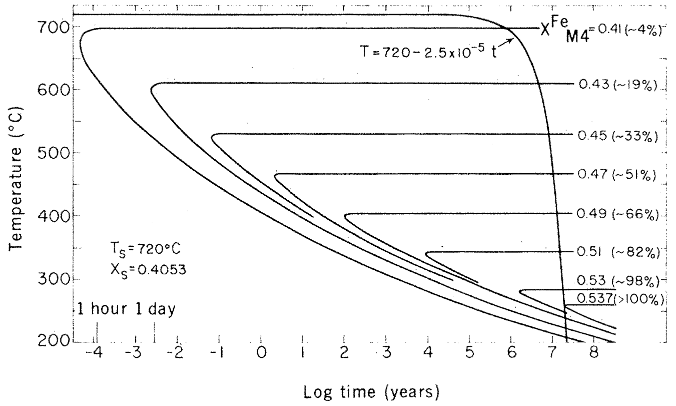

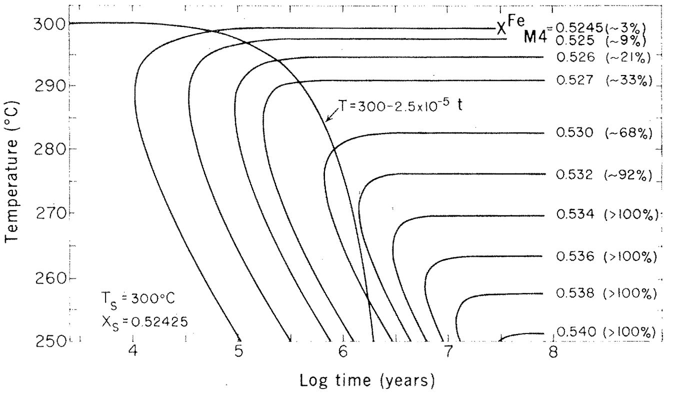

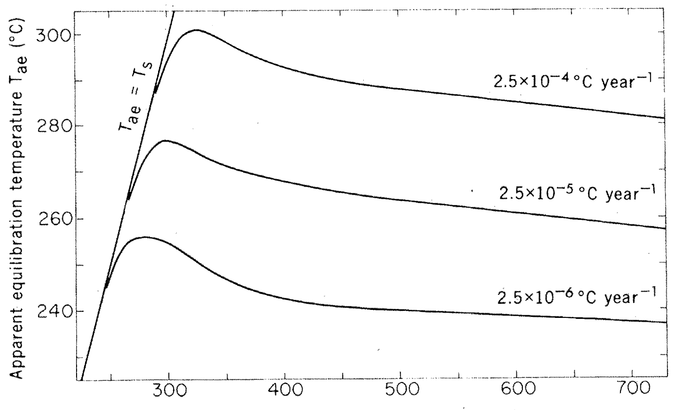

Fig. 1 (upper left). Time-temperature-percentage transformation plot for anthophyllite crystallized at 720°C ($X_s = 0.4053$). Also plotted is the model cooling of a rock taken as T (in degrees centigrade) $= 720 - 2.5 \times 10^{-5}t$. The equilibration temperature of the natural sample is 270°C ($X^{\mathrm{Fe}}{}_{\mathrm{M4}} = 0.533$). Numbers in parentheses refer to the percentage of ordering, from $X_s = 0.4053$ (0 percent) to 0.5327 (100 percent, natural sample) and are defined by

$$\frac{X^{\mathrm{Fe}} - X^{\mathrm{Fe}}{}_{\mathrm{M4,s}}}{X^{\mathrm{Fe}}{}_{\mathrm{M4,nat}} - X^{\mathrm{Fe}}{}_{\mathrm{M4,s}}} \times 100$$

The horizontal portion of each percentage transformation curve refers to the time in excess of that required to achieve equilibrium at a given temperature. Fig. 2 (upper right). Time-temperature-percentage transformation plot for anthophyllite crystallized at 300°C ($X_s = 0.52425$). See also the legend to Fig. 1. Fig. 3 (left). Plot of the apparent equilibration temperature T_{ae} as a function of the crystallization temperature T_s for three distinct linear cooling rates of the rock. The straight line corresponds to a model where $T_{ae} = T_s$.

Table 2. Disordering rate constants, k_{4-123}, where $K°_{123-4} = k_{123-4}/k_{4-123}$, determined for the natural anthophyllite at 500° and 550°C and calculated activation energies for disordering, E_{aD}.

Experiments	k_{4-123} (year^{-1})		E_{aD} (kcal)
	550°C	500°C	
Ordering	37.8432	3.3112	61.6
Disordering	5.0458	0.57816	54.8

These kinetic results portray a distinct pattern of the order-disorder relationship in anthophyllite as compared with other chain silicates: The temperature dependence of the rate constants is much greater (the activation energy for disordering in orthopyroxenes is ~20 kcal/formula unit), and, although both rate constants must decrease with decreasing temperature, the rate constant for disordering must decrease more than that for ordering. The temperature dependence of the rate constants therefore explains the data at 550°C, which show that equilibrium is not attained by disordering within the time scale for equilibrium ordering. Likewise it follows that a disordering experiment at 400°C for 907 hours does not show any change in the Fe^{2+}-Mg distribution. In fact, a change in X^{Fe}_{M4} of 0.001 at this temperature would require a run duration of some 4 years. From these kinetic results, there is no evidence for a high-temperature thermal barrier as previously anticipated, and the degree of ordering in the natural anthophyllite can be quantitatively interpreted in terms of the measured rate constants. Of course, at very low temperatures the ordering process will be terminated owing to slow reaction kinetics after ~10^7 years.

From the rate constants the X^{Fe}_{M4} values that are attained after a given time interval at a given temperature can be calculated, provided that the X^{Fe}_{M4} of the starting material is known. Figure 1 shows such a time-temperature-percentage transformation diagram plotted on a logarithmic time scale and also includes a model cooling history of a rock in terms of temperature and time. From a variety of possible cooling paths for this rock a linear cooling rate of 2.5×10^{-3}/°C year^{-1} is shown, estimated from the closing temperatures of muscovite and biotite and their apparent Rb-Sr age difference (for example, see *15*). From this diagram it might be concluded that the anthophyllite orders completely down to some 260°C and attains an X^{Fe}_{M4} value of 0.537 after ~10^7 years. The inferred cooling history for anthophyllite refers of course to a rapid quench from the crystallization temperature (taken as close to the upper stability limit for anthophyllite, ~720°C in Fig. 1) to the temperature under consideration. In this model the cooling path of the rock is significantly longer than the equilibrium ordering path for anthophyllite, as can be seen in Fig. 1 from the minimum times for equilibrium at successively lower temperatures.

However, the minimum ordering temperature will be different from that deduced from Fig. 1 for different crystallization temperatures. For example, if complete intracrystalline equilibrium is assumed at 300°C and the rock is then cooled with the same linear temperature-time gradient as above (Fig. 2), the lowest X^{Fe}_{M4} value that might be attained is between ~0.531 and 0.532 at 268°C, indicating an apparent equilibration temperature T_{ae} of 277°C. Thus, in the temperature range of interest a nearly equilibrated crystal orders more slowly than an unequilibrated phase, and the limiting X^{Fe}_{M4} values derived from these two specific rock-cooling models represent maximum or minimum apparent equilibration temperatures, respectively. Of course, in a model where the sample is held at the crystallization temperature and then quenched to room temperature, the crystallization temperatures would themselves be the apparent equilibration temperatures.

From models similar to those inferred in Figs. 1 and 2 but with different initial X^{Fe}_{M4} values corresponding to different crystallization temperatures T_s, it can be shown that the rate constants of the exchange process together with the X^{Fe}_{M4} of the natural crystal impose limits on the rate of cooling of the rock. In Fig. 3 the apparent minimum equilibration temperatures have been evaluated for three different temperature-time gradients and are plotted as a function of the crystallization temperature. For a given cooling rate, all values of T_s between $T_{ae} = T_s$ and the apparent equilibration temperature in the natural sample would be permissible. The observed T_{ae} of 270°C in the Rabbitt anthophyllite thus indicates a *maximum* linear cooling rate of ~1×10^{-4} °C year^{-1} for all values of T_s within the anticipated stability field for this particular composition. This value might be subject to an error of about one order of magnitude, however, because it depends on the uncertainty of the T_{ae} value and thus on the invariancy of the $\Delta G°_{ex}$ with temperature.

In conclusion, the kinetic results presented here imply that the measured T_{ae} values in natural anthophyllites directly reflect the cooling rate of rock system. Furthermore, it can be inferred that the time-temperature-percentage transformation plots of coexisting chain silicates will ultimately define the specific rock-cooling path during the later stages of the cooling history.

FRIEDRICH A. SEIFERT
Mineralogisches Institut,
Universität Kiel,
2300 Kiel, Germany

DAVID VIRGO
Geophysical Laboratory,
Carnegie Institution of Washington,
Washington, D.C. 20008

References and Notes

1. D. Virgo and S. S. Hafner, *Mineral. Soc. Am. Spec. Pap. 2* (1969), p. 67.
2. K. Schürmann and S. S. Hafner, *Nat. Phys. Sci.* **231**, 155 (1971).
→ S. Ghose and J. R. Weidner, *Earth Planet. Sci. Lett.* **16**, 346 (1972).
4. R. F. Mueller, *Am. Mineral.* **55**, 1210 (1970).
5. S. S. Hafner and D. Virgo, *Geochim. Cosmochim. Acta* **3** (Suppl. 1), 2183 (1970).
6. J. C. Rabbitt, *Am. Mineral.* **33**, 263 (1948).
7. P. Robinson, M. Ross, H. W. Jaffe, *ibid.* **56**, 1005 (1971).
8. L. W. Finger, *Carnegie Inst. Washington Yearb.* **68**, 283 (1970).
9. F. Seifert, unpublished data.
10. S. S. Hafner and S. Ghose, *Z. Kristallogr.* **133**, 301 (1971).
11. The assignment of 0.045 Ca per M4 site alters the measured rate constant by less than 1 percent.
→ R. F. Mueller, *J. Phys. Chem. Solids* **28**, 2239 (1967).
13. The constant C_0 equal to 0.026 is omitted in these calculations.
14. F. Seifert and D. Virgo, *Carnegie Inst. Washington Yearb.* **73**, 405 (1974).
15. E. Jäger, E. Niggli, E. Wenk, *Beitr. Geol. Karte Schweiz, Neue Folge* **134**, 67S (1967).

6 February 1975; revised 15 April 1975

Forest Fire: Effects on Phosphorus Movement to Lakes

Abstract. *After a wildfire in the virgin forest of a lake-watershed region in northeastern Minnesota, the phosphorus concentration in the runoff was elevated for 2 years and decreased in the third year. However, there was no increase in the phosphorus concentrations of a lake and its input stream. This indicates that, under similar circumstances, controlled burning will not damage streams or lakes by elevating phosphorus levels.*

Does fire in a forested watershed release sufficient nutrients to stimulate eutrophication of streams and lakes? This question needs to be answered because new forest management policies are being introduced which would allow wildfires to burn in wilderness areas and would use fire as a tool to maintain natural species compositions (*1*). These policies indicate recognition that many existing forests are products of wildfires (*2*). The popular message of "Smokey Bear," that fire destroys for-